

# **Rapid Kimberlitic Fluid Extraction from the Lithospheric Mantle**

**I.J. Basson \***

**Department of Geological Sciences  
University of Cape Town, Rondebosch, 7701**

**H. Jelsma**

**CIGCES, Department of Geological Sciences  
University of Cape Town, Rondebosch, 7701**

**G. Viola**

**Department of Geological Sciences  
University of Cape Town, Rondebosch, 7701**

**( \* Presenting )**



## Objectives

- Summarize the sequence of events operative during southern African kimberlite intrusion
- Merge recent models on a number of apparently unrelated features (plate motion vectors, lithospheric mantle fabrics and preferential mantle melt accumulation)
- Ultimately establish a means by which the combined effects of these processes can be modelled



# Southern African Kimberlites

Carbonatite/kimberlites become more abundant from the Proterozoic onwards, and remarkably more abundant **from 600 Ma onwards** (e.g. Janse, 1985)

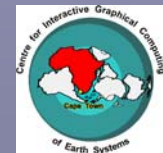
Post-Pan-African **peak in kimberlite volcanism** occurred in the mid-Cretaceous (**approx. 124-83 Ma**) in southern Africa, North America, Brazil and Siberia (e.g. Janse, 1985; Haggerty, 1994)

A total of **4 main events are proposed for southern Africa** (e.g. Dawson, 1986; Skinner *et al.*, 1992))

Mesozoic southern African kimberlites are divided into 2 groups on geochemical and mineralogical grounds: Group II (mainly **145-115 Ma**) and Group I (mainly **95-80 Ma**) (Smith *et al.*, 1985)

Group I are “normal” ilmenite-bearing kimberlites with distinct Pb, Sr and Nd isotopic ratios, intruded at approximately 1600 Ma, 1200 Ma, 500 Ma (e.g. Smith *et al.*, 1985)

Group II kimberlites are highly-micaceous and ilmenite-poor (e.g. Smith *et al.*, 1985)



# Carbonatite-Kimberlite Structural Relationship?

(q.v. geochemical link - Harmer, 1998)

## **Wolley (1989):**

*“...localization of carbonatitic activity over time / several periods suggests lithospheric control”*

*“The location and genesis of carbonatites is determined in some way by the physical and/or chemical properties of the lithospheric plate”*

## **van Straaten (1989):**

*“...carbonatite magmatism is related to recurrent reactivation of older structures and argues for a control by crustal rather than mantle processes.”*



# Cretaceous Events

- Increased mid-Cretaceous mantle convection (“**superplumes**”)
- **Accelerated plate motion** coinciding with the arrival of the Parana, Etendeka, Gondwana and Ontong Java Superplumes, representing a deep-sourced heat pulse from the CMB (+“Normal” geodynamo field orientation between 120 and 80 Ma) (e.g. Haggerty, 1989, 1994)
- **Higher mean mantle Potential Temperatures**, temperatures skewed towards higher values and a greater degree of temperature variance, increased rate of global mantle convection and plate motion (e.g. Larson, 1991; Ricciardi & Abbott, 1996)

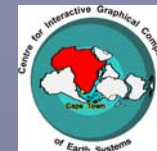
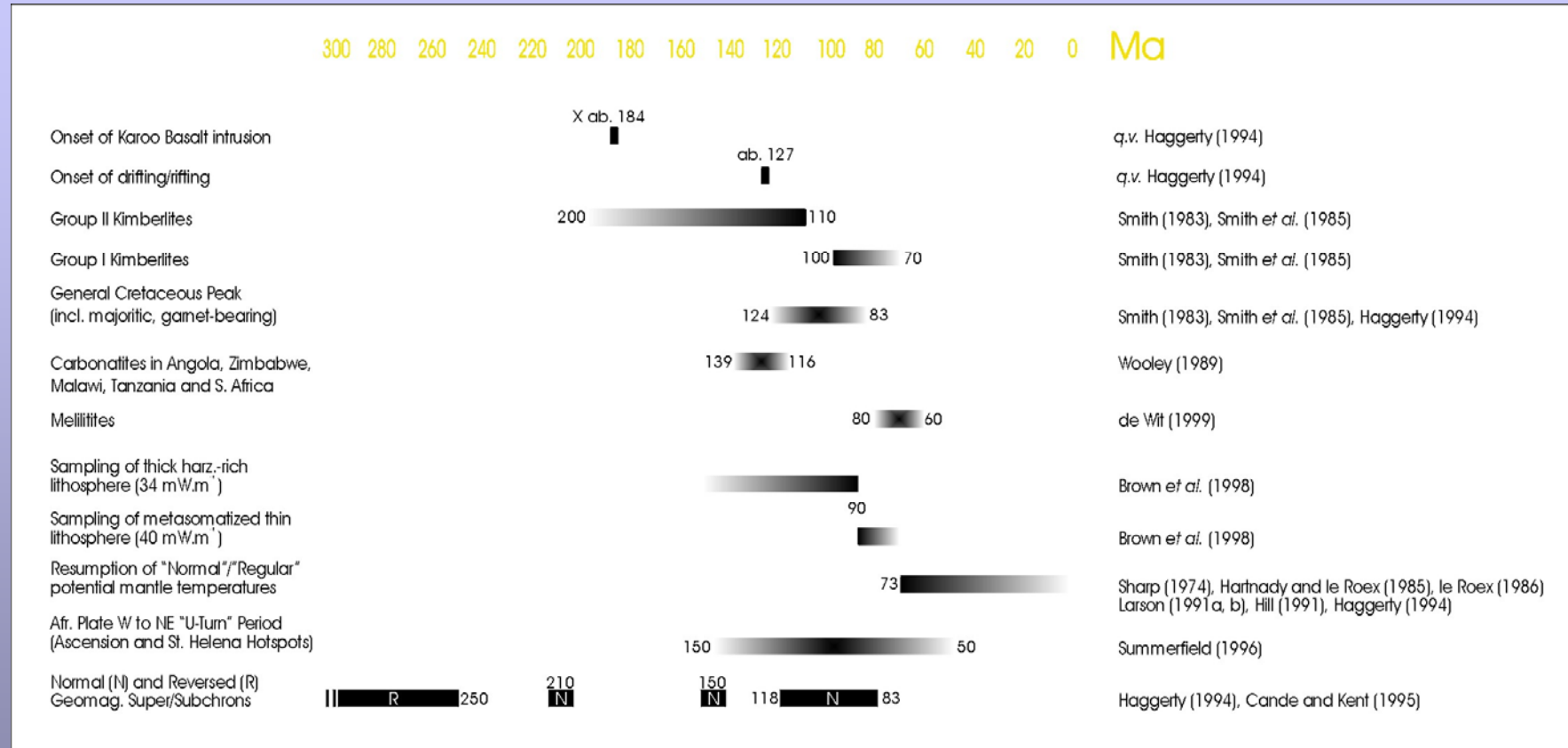
Kimberlites erupted **prior to 90 Ma** (nominally Group II types) sampled **harzburgitic material from depths between 180 and 140 km**, within a **210-220 km thick lithosphere** ( $34 \text{ mW.m}^{-2}$ ). Post-**90 Ma** kimberlites sampled a **highly metasomatised lithosphere**, with a raised geotherm of  $40 \text{ mW.m}^{-2}$ , from shallower depths (**170 km**) (e.g. Brown *et al.*, 1998)

- **Extreme thinning of the MBL**, significantly raised geotherms and uplift driven by buoyancy, resulting from a decrease in the density of the lithospheric roots (e.g. Brown *et al.*, 1990, 1998)
- **Uplift and denudation**, constrained by existing apatite fission-track (FT) dating (summary by Summerfield, 1996)
- **“Vertically coherent deformation”** wherein changes in the lithospheric mantle are reflected in the overlying lithosphere (Silver *et al.*, 2001)

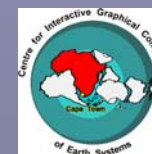
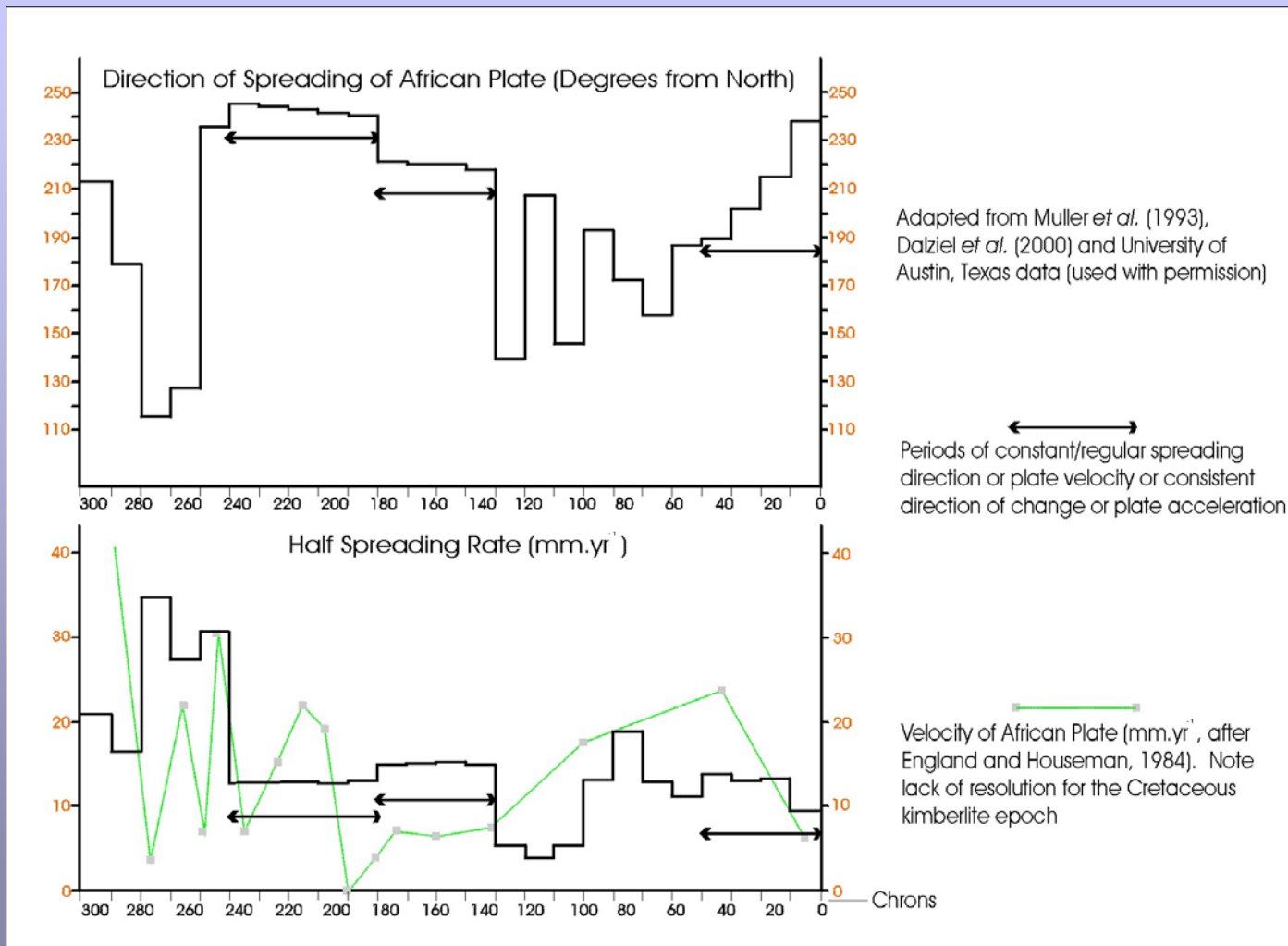
( A more **regular potential mantle temperature** resumed **after ca. 73 Ma** or just after the end of the mid-Cretaceous (e.g. Larson, 1991; Ricciardi & Abbott, 1996) )



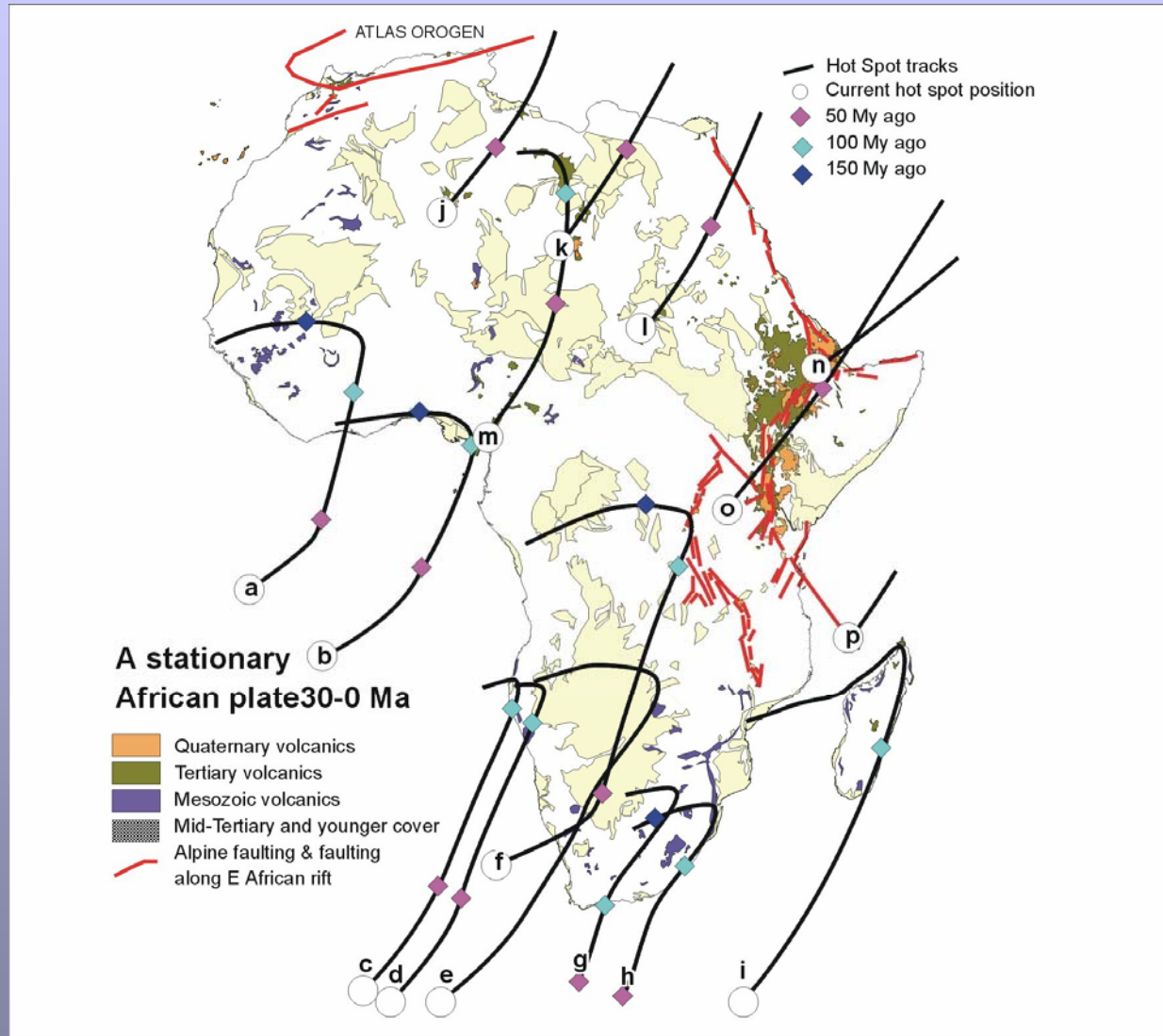
# Cretaceous Event Summary



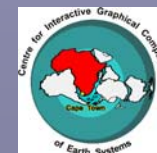
# Cretaceous Spreading



# Cretaceous Plate Motion



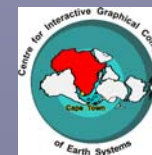
Adapted from Summerfield (1996), "demolished" by Burke (1996)





## Mantle Fabrics

- A N50E-trending shear wave splitting (fast) polarization direction (e.g. Vinnik *et al.* 1995; Fouch *et al.* 2001)
- “**Central EET high**”, an “arcuate saddle-like maximum (average width  $\gg$  350 km, average magnitude  $\gg$  70 km) from northeast to southwest [which] dominates the EET map” (Doucouré & de Wit, 1998)
- Central EET high coincides with **present velocity vector of the African plate**, N40-45E at 14-20 mm.yr<sup>-1</sup> (Online Goddard Space Flight Center, VLBI Solution KB2001 of Version 01)
- Trend coincides with **the spatial** (but not temporal?) **Venetia-Premier-Kimberley kimberlite trend**, and NE-SW lith. extensional stress of up to 8 MPa at 125 km depth (e.g. le Roex, 1986; Doucouré & de Wit, 1998)
- **Two mutually orthogonal lattice preferred orientations pervasive throughout the Ivrea Zone** (LPO) **1**) strongly plastically deformed and sheared with a high degree of deformation/recrystallization and **2**) c.g., commonly garnet-bearing, without microstructural signs of high temperature, stress or deformation rates; equilibrated at normal continental geotherms between 60 and 130 km (Ben-Ismaïl *et al.*, 1998, 2001)
- The [100], [010] and [001] axes in olivine become **aligned** with longest, shortest and intermediate strain ellipsoid axes; max. principal stress direction ( $\sigma_1$ ) sub-perpendicular to 010 faces of olivine crystals (*q.v.* oceanic crust, [100] axes oriented sub-parallel to spreading direction in the upper mantle – Ribe, 1989, Vinnik *et al.*, 1995, Waff & Faul, 1992)
- Vinnik *et al.* (1995) suggested **present “flow”** or shearing of sublithospheric mantle of the Kaapvaal Craton (e.g. Ribe, 1989) is **inherited from Precambrian** or related to consistent plate motion in the Jurassic period; *q.v.* North American and Australian Plates (e.g. Debayle and Kennett, 2000)



# Fluid Ascent Rates

Reference	Basis	Upper mantle-lower crust transit $\Delta Z = 100-10 \text{ km}$ fluid velocity (km.hr <sup>-1</sup> ) mins transit hours transit	Transit speed within the upper crust as dykes $\Delta Z = 10-1 \text{ km}$ fluid velocity (km.hr <sup>-1</sup> ) mins transit hours transit	Fluidised intrusion as diatremes $\Delta Z = 1-0 \text{ km}$ fluid velocity (km.hr <sup>-1</sup> ) mins transit hours transit
McGetchin (1968) Model F	Fluid dynamics, Bernoulli equation, Newtonian flow in pipe	<u>43</u> 125 <b>2.09</b>	-	-
McGetchin (1968) Model F	Fluid dynamics, Bernoulli equation	-	<u>122</u> 4 <b>0.07</b>	-
McGetchin (1968) Model F	Fluid dynamics, Bernoulli equation	-	-	(482) (0.1) <b>0.002</b>
Ferguson (1970)	Flow in kimberlite dykes	-	<u>72</u> 7.5 <b>0.12</b>	-
Currie and Ferguson (1970)	Structural analysis, propagation of lamprophyre dykes	-	<u>72</u> 7.5 <b>0.12</b>	-
McGetchin and Ullrich (1973)	Fluid dynamics	<u>72-90</u> <u>75-60</u> <b>1.25-1</b>	-	-
McGetchin <i>et al.</i> (1973); Ullrich (1969)	Fluid dynamics and phase relations of carbonatitic and kimberlitic fluids	<u>200-20</u> 29.7-297 <b>0.5-4.95</b>	-	-
Smyth and Hatton (1977)	Preservation of diamond and coesite in lower transit area	<b>Several hours</b>	-	-
O'Hara <i>et al.</i> (1971); Mori and Green (1975)	Equilibration of mechanical mixture of water and mantle minerals	-	<b>100-4</b> NA <b>1-24</b>	-
Mercier (1979)	Recrystallization rates of strain-free neoblasts which replace strained crystalline mantle material	-	<b>40-70</b> 150-85 <b>2.5-1.4</b>	-
McCallister <i>et al.</i> (1979)	Exsolution in clinopyroxene	-	<b>11-25</b> 545-240 <b>9.1-4</b>	-
Ganguly (1981)	Kinetic diffusion calculations on pyroxenes and Ca-poor amphiboles	-	<b>0.7-0.01</b> NA <b>144-8544</b>	-
Mitchell (1979), Canil, Fedortchouk (1999), Rutherford and Gardner (2000)	Mafic dyke mineralogy, garnet dissolution rates (based on 160km thick lithosphere of Mitchell <i>et al.</i> , 1998)	-	<b>16-160</b> 375-38 <b>6.3-0.6</b>	-

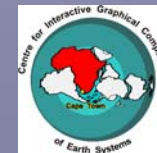
Mean of  
70 km.hr<sup>-1</sup>

Lithosphere  
transit in  
<3hrs




# Mantle Fluid Accumulation - I

- The measured effective dihedral angles for basaltic melt in contact with olivine range from 20° to 50° natural melt forms an **interconnected network** for a wide range in melt fractions and dihedral angle
- **Increasing melt fraction and increasing grain size** results in an **increase in the size and aspect ratio of melt pockets**, (sub-parallel to olivine 010); occurs in hotspot conditions (e.g. Daines & Kohlstedt, 1996)
- The melt pocket aspect ratio (long : short axis ratio) is **highest at low melt fractions** (0.01 to 0.02: *q.v.* partial melt fractions of kimberlitic/carbonatitic magmas or melt fraction required for 50% of grain boundaries to be wetted) & higher melt fractions (>0.18) (e.g. Riley *et al.*, 1990; Hirth & Kohlstedt, 1995)
- Melilititic, nephelinitic, carbonatitic and kimberlitic melts are **highly mobile** in the upper mantle/lithospheric mantle at very small melt volumes (<1%) (e.g. Watson & Brenan, 1987; Harmer, 1998)
- Ave'Lallemant and Carter (1970): **preferred orientations of melt** in an anisotropically deformed lherzolite:melt system; ■ Bussod and Christie (1991): **preferred orientation of melt 'slots'** along recrystallized grain boundaries at 30° to  $\sigma_1$  in partially molten lherzolite under hydrous conditions; ■ Daines and Kohlstedt (1996): samples deformed at differential stresses greater than 100 MPa exhibited **more melt in pockets at 15-20° to  $\sigma_1$** ; such pockets were a factor of 2 larger and more elongate than those perpendicular to  $\sigma_1$

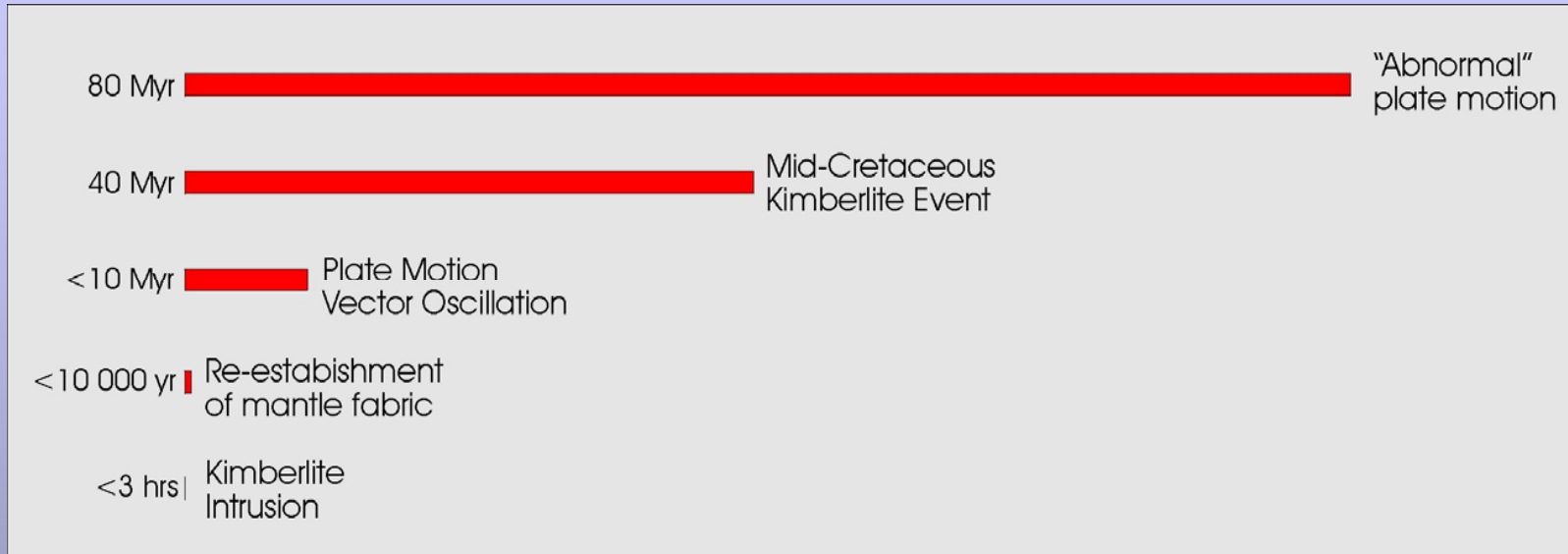


## Mantle Fluid Accumulation - II

- At fast spreading ridges (90 mm.yr<sup>-1</sup> half rate), with olivine bulk diffusion of  $3 \times 10^{-11}$  cm<sup>2</sup>.s<sup>-1</sup>, complete equilibration of grains with a 1.5 cm radius (*q.v.* Thaba Putsoa kimberlite mantle xenoliths) occurs in  **5500 years** (Waff & Faul, 1992)
- Degree of melt-preferred orientation relates to the imposition of a (relatively high) **differential stress**, rather than strain rate/total cumulative strain
- Surplus melt pockets primarily occur and may be **expelled** where the semi-molten rock contains more than its minimum energy porosity, a situation that arises during the **deforming/non-static or non-hydrostatic case**
- w.r.t. CO<sub>2</sub>-H<sub>2</sub>O fluids: the absolute necessity of **rapid deformation** to overcome the rate of wetting equilibration i.e. "If  $\Theta > 60^\circ$  then the only mechanism available for fluid penetration into non-porous rocks is hydrofracture" (Watson & Brenan, 1987)



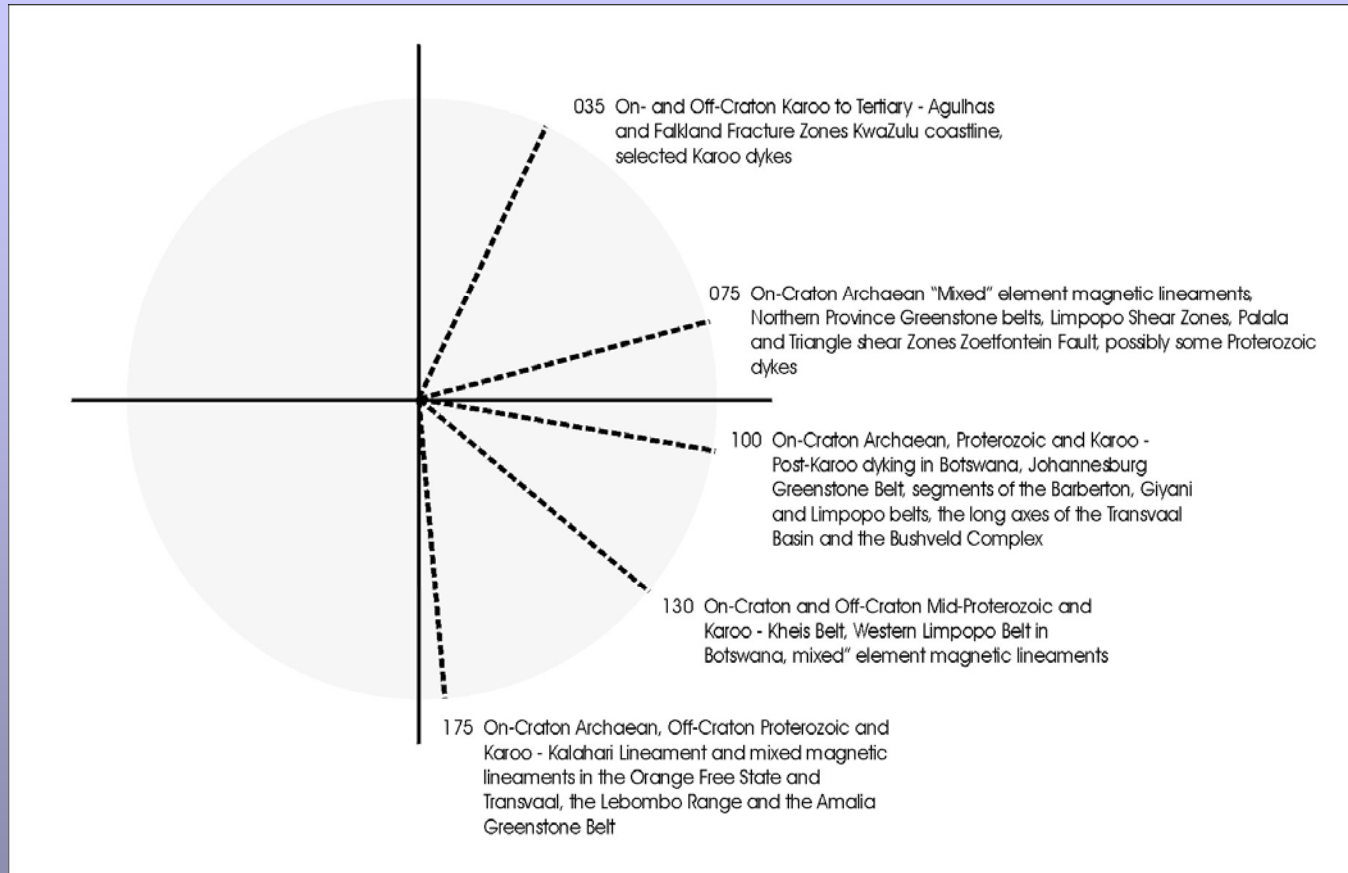
# “Hierarchy” of Periodicity?



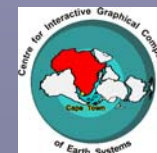
(V. Schematic)



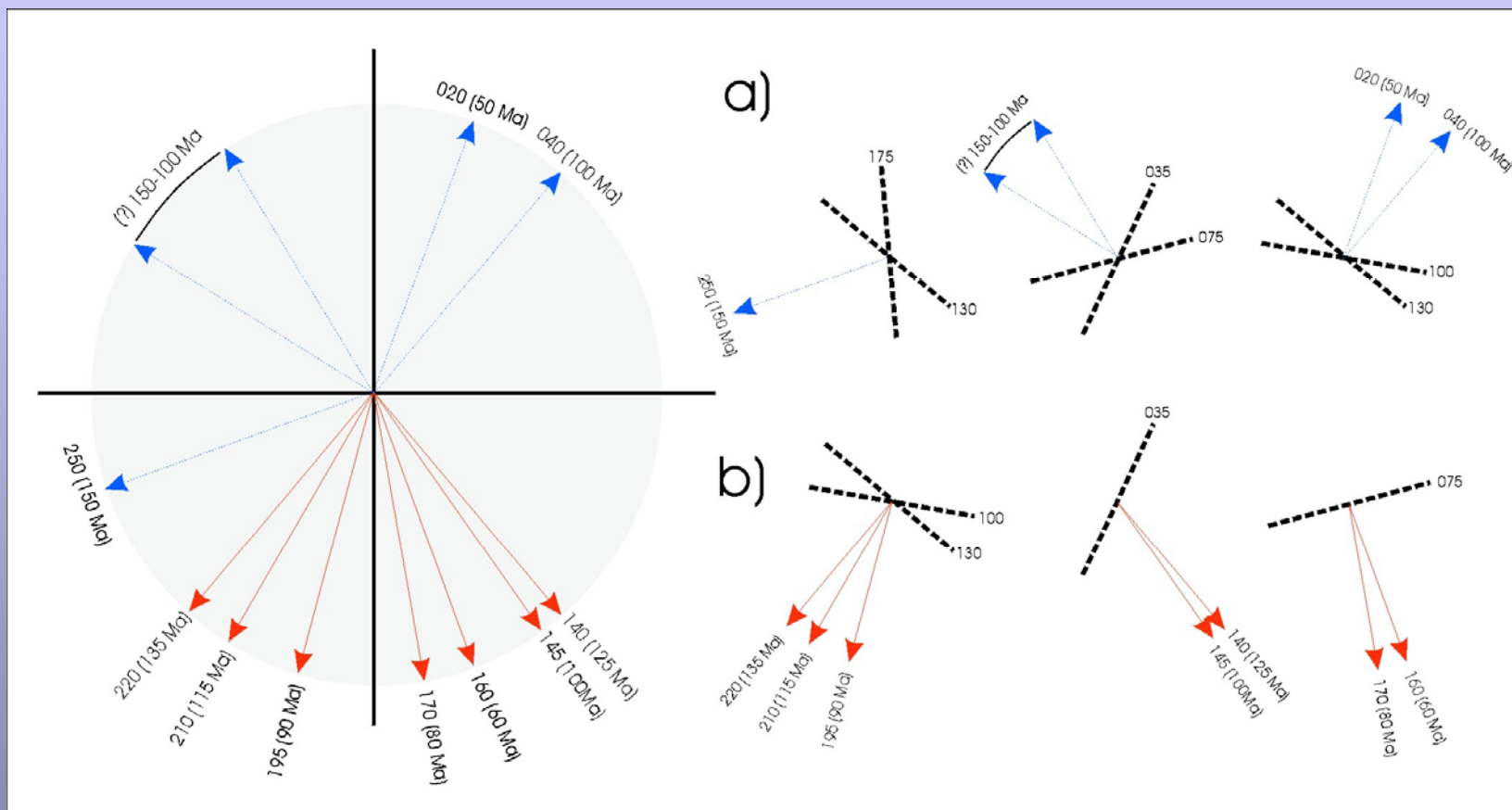
# Kimberlite Trends?



Summary of kimberlite trends (Fry analysis of 780 S.A. kimberlites),  
from Verncombe and Verncombe (2002)



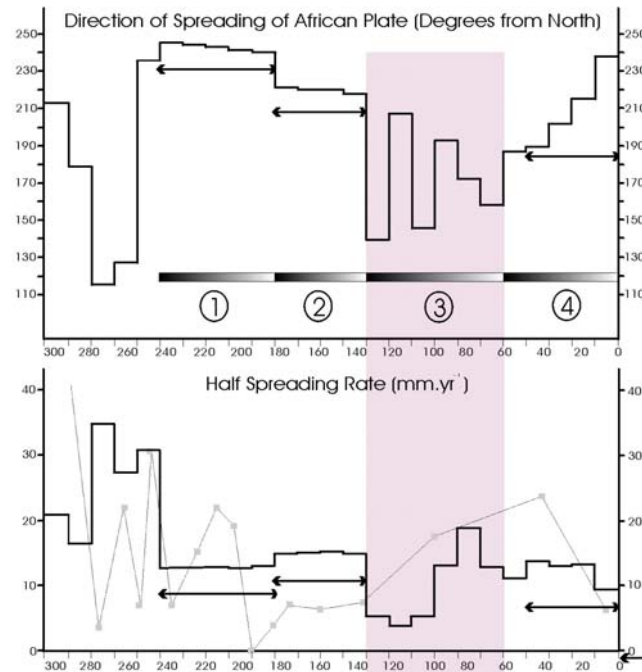
# Interaction: Kimberlite Trends and Vector Changes (a means for repeated kimberlite intrusion in the same area?)



Combination of Verncombe and Verncombe (2002) kimberlite trends with data from

- a) Summerfield (1996) – continental “U-Turns”
- b) University of Austin, Texas data – spreading vector oscillations

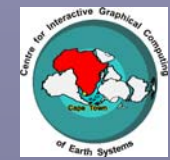
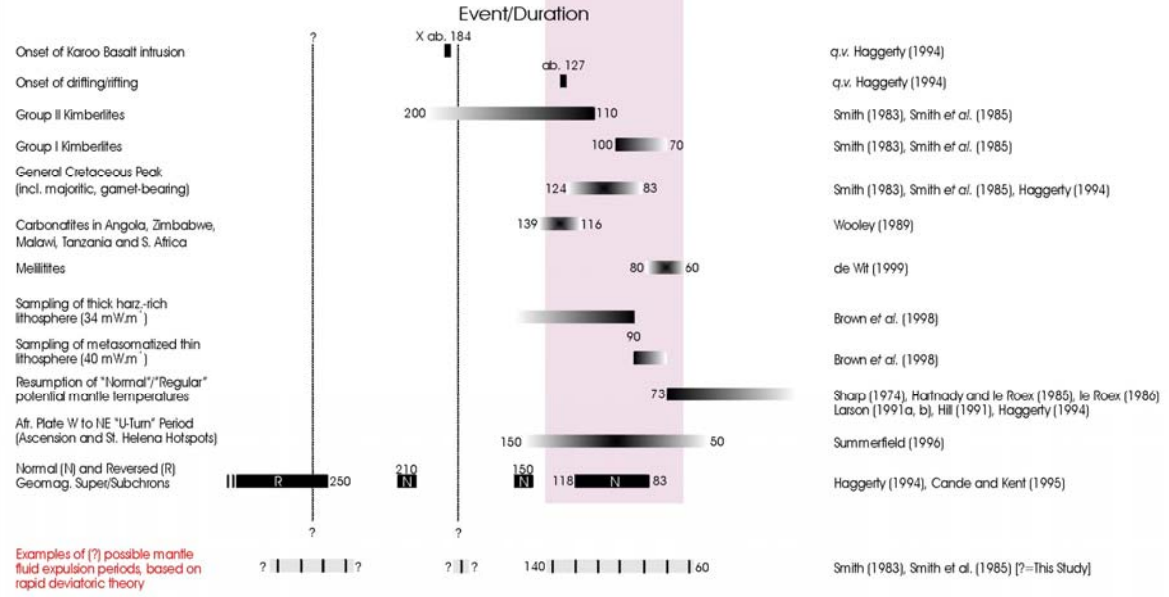




Adapted from Muller *et al.* (1993), Dalziel *et al.* (2000) and University of Austin, Texas data (used with permission)

←→ Periods of constant/regular spreading direction or plate velocity or consistent direction of change or plate acceleration

— Velocity of African Plate (mm.yr<sup>-1</sup>), after England and Houseman, 1984. Note the lack of resolution for the Cretaceous kimberlite epoch





## Proposed Model?

- Development of an LPO/preferred melt orientation in the 240-140 Ma period due to consistent spreading direction, interrupted at approximately 180 Ma (Karoo Basalt event at approx 184 Ma) by a minor 20° spreading vector change). Approx. 220°-trending melt pockets.
- Major plate spreading vector switch, to 140° at 125 Ma and a dramatic drop in spreading rate. Imposition of a new shearing direction ( $\sigma_1$ ?) at a high angle to existing fabric. Rapid re-establishment of a stable effective dihedral angle and extremely rapid (“catastrophic”?) propagation of suitably oriented crustal structures into the upper mantle. Initiation of carbonatite intrusion in southern Africa at approximately 139 Ma, the start of the Mid-Cretaceous peak, Group II kimberlite activity and the sampling of thick, harzburgite-rich lithosphere with 34 mW.m<sup>-2</sup> geotherm.
- Repeated switches in plate spreading vector interrupted only by a sudden redoubling of the half spreading rate at approximately 100 Ma, coinciding with the start of Group I kimberlite magmatism, the sampling of metasomatised thinned lithosphere with 40 mW.m<sup>-2</sup> geotherm and the approximate midpoint of the Mid-Cretaceous kimberlite intrusion event.
- The resumption of a more regular spreading velocity and a regularly changing (rotating) plate spreading vector heralded the conclusion of the Mid-Cretaceous event, coinciding with the resumption of more “normal” geotherms at 73 Ma and melilitite intrusion from 80-60 Ma.



## The Key to Structural Modelling?

The intrusion of kimberlites into various structures in the Kaapvaal Craton should perhaps be viewed as the result of their *tectonic extraction* from the mantle in areas that contain a ready source of kimberlitic or other low-viscosity fluids, rather than an “active” event whereby extremely small volumes of “intruding” kimberlitic magma are able to “overcome” the strengths and stresses of the Kaapvaal Craton

